RSC Advances

ROYAL SOCIETY OF CHEMISTRY

www.rsc.org/advances

Cardanol Benzoxazines – Interplay of Oxazine Functionality (Mono to Tetra) and Properties

Swapnil Shukla,[a] Arup Mahata,[b] Biswarup Pathak[b] and Bimlesh Lochab[a†]

[a.] *Department of Chemistry, School of Natural Sciences, Shiv Nadar University, Gautam Budh Nagar, Uttar Pradesh 203207, India.*
[b.] *Discipline of Chemistry, School of Basic Sciences, Indian Institute of Technology (IIT) Indore, M. P., India.*
† Corresponding Author *Telephone: +91-9899915584. Fax: +91-1202663810. E-mail: bimlesh.lochab@snu.edu.in.

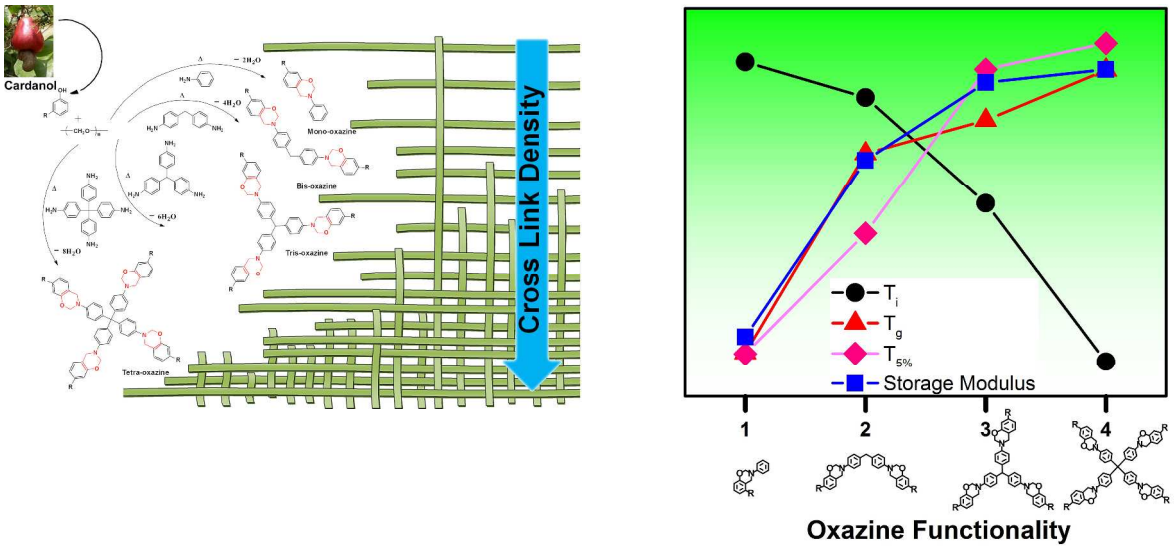

Cardanol, an agrowaste - solventless synthesis and processability of benzoxazine monomers.

Tailoring the polymer properties as a function of oxazine functionality in the monomers.

Journal Name

ARTICLE

Cardanol Benzoxazines – Interplay of Oxazine Functionality (Mono to Tetra) and Properties

Received 00th January 20xx,
Accepted 00th January 20xx

DOI: 10.1039/x0xx00000x

www.rsc.org/

Swapnil Shukla,[a] Arup Mahata,[b] Biswarup Pathak[b] and Bimlesh Lochab[a†]

Cardanol, a sustainable origin phenol, was utilized as a reactive diluent to mediate solventless Mannich-type condensation reaction with paraformaldehyde and primary aromatic amines to form a homologous series of benzoxazine (Bz) monomers namely C-a, C-ddm, C-trisapm and C-tetraapm which differ in their degree of oxazine functionality as mono-, di-, tri- and tetra-oxazine respectively. A strong correlation is reflected between the number of oxazine rings in the monomer and the polymerization behavior, thermo-mechanical transitions, and properties of the polybenzoxazine synthesized. The monomer structure was confirmed by FTIR, ^{1}H-, ^{13}C-NMR spectroscopy and mass spectrometry. The curing, rheological, thermo-mechanical and thermal properties were determined using DSC, FTIR, rheometer, DMTA, LSS and TGA studies. The curing characteristic due to ROP of Bz monomers was supported both by DSC and FTIR studies. The presence of neighboring oxazine group in monomers (C-a to C-tetraapm) strongly attenuates the curing temperature (T_i = 225-140^{o}C), enhances T_g, thermal stability, and mechanical properties. Interestingly, DFT calculations also supported the lowest curing temperature for highest oxazine functionality monomer (C-tetraapm). The interplay between the degree of oxazine functionality in the monomer; extent of H-bonding and crosslink density values in sustainable origin synthesized polybenzoxazines is suggested. The thermoset showed an increasing trend (PC-a< PC-ddm<PC-trisapm<PC-tetraapm) in T_g (58-109^{o}C), thermal stability (355-391^{o}C), char yield (13-37%), LOI (23-31) and storage modulus (3.6-66.5MPa) values. The monomers are liquid to semi-viscous paste at room temperature and showed potential for solventless processing in adhesive applications.

KEYWORDS: Cardanol, Biobased benzoxazines, solventless synthesis, highest functionality, DFT calculations

Introduction

Addition-cure phenolic thermosets, polybenzoxazines (PBz) have gained prominence in the past decade as an alternative to conventional phenol formaldehyde resins which are associated with poor shelf life of the precursors, requirement of catalyst for polymerization, evolution of volatiles and volumetric shrinkage during the curing reaction. This new class of phenolics exhibit better mechanical and thermal properties with a simultaneous molecular design flexibility. [1-2] In addition to better thermomechanical properties, they are also an attractive candidate due to the simplicity of the reaction conditions, which involves Mannich-like condensation reaction of phenol, formaldehyde and amine. The structure of phenol and amine can be altered, designed and functionalized to synthesize benzoxazine monomers (Bz) to offer a wide range of applications.[3-5] In the past, the synthesis of Bz has remained dependent on exhaustible petroleum sources with several associated drawbacks limiting their large scale commercialization. Among these, the majority of petro-based Bz monomers possess difficulty in processing into thin films due to their rigidity in the backbone of the basic monomer unit and poor solubility in solvents. Till now several modifications have been attempted to enhance properties of PBz resins and counter associated disadvantages which include introduction of different functionalities, synthesizing blends, addition of fillers etc.[6-10] In the current scenario, naturally occurring phenolic sources are being explored as a substitute for the petro-phenol in benzoxazine monomer synthesis. Their sustainability and presence of other functional groups provide avenues for further structural modification and impart low viscosity which assists solventless synthesis and processing. Also, they offer an intriguing new direction to create novel materials from bio-origin to meet the growing demands of reduced dependence on non-renewable fossilized reserves. However, to compete for the larger petro-based phenolic polymer market a major initiative is required for the adoption of sustainable phenolic sources for utility-scale polymer

[a] *Department of Chemistry, School of Natural Sciences, Shiv Nadar University, Gautam Budh Nagar, Uttar Pradesh 203207, India.*
[b] *Discipline of Chemistry, School of Basic Sciences, Indian Institute of Technology (IIT) Indore, M. P., India.*
† Corresponding Author *Telephone: +91-9899915584. Fax: +91-1202663810. E-mail: bimlesh.lochab@snu.edu.in.
Electronic Supplementary Information (ESI) available: [details of any supplementary information available should be included here]. See DOI: 10.1039/x0xx00000x

applications. This requires a significant understanding and systematic analysis of bio-based phenolic polymers properties to tap their usage. Few publications[11] have reported the utilization of bio-origin phenol such as eugenol,[12-14] vanillin,[15-17] urushiol,[18-19] rosin,[20] and lignin source phenols such as guaiacol,[21] ferulic, coumaric, phloretic acid[22] to realize their potential from synthetic aspect. However, their food based origin, latent toxicities, higher curing temperature, complex structure and challenges in mass scale production has led to innovative exploration of cardanol as a phenolic substitute. The advantages of cardanol include non-food agro waste origins, commercially viable extraction process and huge tonnage production at cheaper exportable prices (US$1.23-2.33/metric tonne).[23] Cardanol, is obtained by vacuum distillation of "cashew nut shell liquid" (CNSL), which is an alkyl phenolic oil contained in the spongy mesocarp of the cashew nut shell from the cashew tree *Anacardium occidentale L.*

Cardanol based Bz monomers require a high temperature for curing (~200-250 °C) which may limit their potential and applicability to a certain extent.[24-28] Both petro- and bio-based monomers polymerize at much higher temperatures rendering them unsuitable for applications demanding low curing temperature. The ring strain in oxazine allows heat mediated ring opening reaction, which is then followed by an autocatalytic polymerization route due to generation of phenolic acidic moieties. The temperature associated with ROP of benzoxazines is lowered either by physical blending with catalyst[29-30] or by chemical modifications.[31-33] Latter involves introduction of electron-withdrawing or electron-donating groups, or acidic groups that can either activate the ring opening or stabilize the intermediates to assist ROP. Recently few reports are published solvent based synthesis of benzoxazine monomers containing three and four oxazine rings using petro-sourced phenols and/or amines.[34-37] Surprisingly, the effect of neighboring group participation of oxazine ring on enhancing benzoxazine autocatalytic polymerization has not been explored so far. To the best of our knowledge, attempts towards establishing the correlation between increasing oxazine functionality in a monomer, and its effect on polymer properties has not been reported.

In this paper, we report a series of benzoxazine monomers synthesized from sustainable origin phenolic compound, cardanol. The monomers designed are structural analogue to cardanol based mono-oxazine which differs in their degree of oxazine functionality to understand the correlation between Bz structure-property in detail. This will provide insight for the potential of biobased benzoxazine monomers, which is still at a nascent stage and requires further systematic study. We hypothesize that the additional tethering of oxazine ring in the monomer may allow lowering of curing temperature due to proton diffusion; intramolecular vs intermolecular and also account for higher cross-linking density due to neighboring groups. These will obviate the need for additional curing/catalyst mediators by physical blending which affect the resin properties.

Experimental

Materials

Cardanol (ρ =0.9272-0.9350 g cm^{-3}; iodine value 250; Acid Value Max 5; Hydroxyl Value 180-190)was procured from Satya Cashew Chemicals Pvt. Ltd. (India), paraformaldehyde, aniline and fuming nitric acid from Fisher scientific, chloroform from Finar, anhydrous sodium sulphate from Chemlabs, sodium borohydride and pararosaniline hydrochloride from CDH, 4,4'-diaminodiphenylmethane, tetraphenylmethane from Alfa Aesar and ethanol from Emsure. All the reagents were used as received.

Characterisation

Fourier Transform Infrared (FT-IR) spectra were recorded on a Nicolet iS5 spectrometer equipped with iD5-ATR accessory, in the range of 4000 to 400 cm^{-1}. ^{1}H-NMR of the samples were recorded on Bruker AC 500 MHz using $CDCl_3$ and $(CD_3)_2SO$ as solvents and tetramethylsilane (TMS) as an internal standard and plotted using Mestrec software. Mass spectrometry analysis was carried out using Agilent HRMS Q-ToF 6540 Series equipped with ESI mode. The curing behavior of monomers was evaluated by Differential Scanning Calorimetry (DSC) (TA instruments Q 20). For each scan, samples (10±2 mg) were enclosed in hermetic aluminium pans and heated from 40°C to 400°C at a heating rate of 10°C/min under nitrogen purge at a constant flow rate of 50 mL/min. Prior to the experiments, the instrument was calibrated for temperature and enthalpy using standard indium and zinc. Thermogravimetric analysis (TGA) of cured monomers was performed with Perkin Elmer Diamond STG-DTA in the temperature range 30 to 700^{o}C and a heating rate of 10^{o}C/min under nitrogen atmosphere at a flow rate of 50 mL/min. Anton Paar Rheometer MCR302-CTD450 was used to perform Dynamic Mechanical Thermal Analysis (DMTA) of the cross-linked polymer sample by applying oscillatory mode with amplitude, γ= 0.5%, angular frequency, ω=10 rad/s and a temperature ramp rate of 2°C min^{-1}.

Preparation of Thermosetting Resins for Lap Shear Strength (LSS) Studies.

Lap shear strength (LSS) of bonded joints on stainless steel (65 x 15 mm^2) plates of roughness (0.14–0.18 μm) was measured in accordance with ASTM standard D1002 on an INSTRON 5582 100 KN tensile testing machine with a crosshead speed of 1.3 mm min^{-1}. For LSS determination, samples were prepared by coating Bz monomers on the overlap area (15 x 15 mm^2) of stainless steel coupons held together by binder clips and oven cured. An average LSS value of five specimens was reported.

Synthesis of Monomers

Synthesis of higher functionality amines

Tris-p-aminophenylmethane (TrisAPM)[38] and tetra-*p*-aminophenylmethane (TAPM)[39] were prepared as per the reported procedure with little modifications. Amine synthesis involved reduction strategies from corresponding salt and nitro precursor to

result in tris- and tetra-*p*-aminophenylmethane, respectively. Synthetic strategies are detailed below.

*4,4',4''-methanetriyltrianiline [Tris-p-aminophenylmethane (***TrisAPM***)].* To a solution of pararosaniline hydrochloride (0.50 g, 1.54 mmol) prepared in ethanol (40 mL), sodium borohydride (0.53 g, 14.00 mmol) was added in two lots with continuous stirring in an ice bath. Reaction continued till complete dissolution of sodium borohydride accompanied by a color change from deep pink to yellow. Reaction was quenched with addition of water (75 mL) and a yellow precipitate of Tris-APM was obtained after simple filtration. Yield 84 %. FTIR-ATR (diamond crystal/cm^{-1}): 3336, 3203, 3029, 1608, 1507, 1267, 815, 770; ^{1}H-NMR (500 MHz, $CDCl_3$, δ ppm): 6.88 (d, 6H, ArH), 6.60 (d, 6H, ArH), 5.24 (s, Ar_3C-H), 3.56 (br, s, 6H,–NH_2); LC-MS (ESI Interface-positive ions): $[M+H]^+$ 290.1651 (290.1613).

*tetrakis(4-nitrophenyl)methane [Tetra-p-nitrophenylmethane (***TNPM***)].*Tetraphenylmethane (2.00 g, 6.24 mmol) was added to mixture of fuming nitric acid (11 mL), glacial acetic acid (6.8 mL) and acetic anhydride (3.8 mL) at -40^{o}C with vigorous stirring. The resultant mixture was stirred for 5h and filtered to give yellow solid which was washed with water, dried and re-crystallized using tetrahydrofuran to give TNPM as yellow crystals. Yield 82%; FTIR-ATR (diamond crystal/cm^{-1}): 3070, 3100, 1605, 1591, 1519, 1493, 1347, 840, 757, 744, 711. ^{1}H-NMR (500 MHz, $CDCl_3$, δ ppm): 8.22 (d, 8H, Ar-H), 7.41 (d, 8H, Ar-H).

*4,4',4'',4'''-methanetetrayltetraaniline [Tetra-p-aminophenylmethane (***TAPM***)].* To a solution of TNPM (1.40 g, 2.79 mmol) in tetrahydrofuran (35 mL), Pd/C (10% Pd, catalytic amount) was added and the reaction mixture was purged with nitrogen followed by hydrogen. Thereafter, the reaction mixture was stirred under hydrogen pressure at room temperature for 3 days followed by filtration over celite to remove Pd/C powder. The filtrate was dried to give TAPM as white powder. Yield: 96%. FTIR-ATR (diamond crystal/cm^{-1}): 3400, 3161, 3022, 1608, 1507, 1267, 803. ^{1}H-NMR (500 MHz, $(CD_3)_2SO$, δ ppm): 6.67 (d, 8H, Ar-H), 6.38 (d, 8H, Ar-H), 4.85 (s, 8H, -NH_2); LC-MS (ESI Interface-positive ions): $[M+H]^+$: 381.2063 (381.2035).

Synthesis of cardanol based benzoxazine monomers. *7-alkyl-3-phenyl-3,4-dihydro-2H-benzo[e][1,3]oxazine* (**C-a**). The monomer C-a was prepared in reference to the procedure.[24] In brief, a mixture of cardanol (5.00 g, 16.61 mol), paraformaldehyde (1.00 g, 33. 22 mmol), aniline (1.51 mL, 16.61 mmol) was gradually heated to 80^{o}C and stirred for an hour, followed by heating at 90^{o}C for 2h. The reaction was indicated by evolution of water and colour changed from yellow to red brown. On cooling, water (10 mL) was added and organic layer was extracted with chloroform (20 mL). The organic layers were combined and washed with NaOH (0.5 N, 100mL) followed by washing with water (3 x 30 mL), dried over sodium sulphate and filtered. The solvent was removed under reduced pressure to give C-a as a red oil. Yield 95%; FTIR-ATR (diamond crystal/cm^{-1}) 3008, 2926, 2854,1626, 1595, 1579, 1350, 1257, 1240, 1116, 1030, 995, and 950; ^{1}H-NMR (500 MHz, $CDCl_3$, ppm): 0.94 (CH_3,t), 1.35 [(CH_2)n, m], 1.85, 2.07 (CH_2CH=, m), 2.59 (CH_2Ar, t), 2.89 [$CH_2(CH=)_2$, m], 4.55 (s, $ArCH_2N$–), 5.05 (–CH=CH–, dd), 5.30-5.40 (m, CH=, CH_2=CH–, –OCH_2N–,–HC=CH_2), 6.60(ArH, s), 6.72(ArH, d), 6.93 (ArH, m), 7.15 (ArH, d), 7.27 (ArH, m); ^{13}C-NMR (125 MHz, $CDCl_3$, ppm): 50.38 ($ArCH_2N$–), 79.47 (–OCH_2N–); LC-MS (ESI Interface-positive ions) $[C\text{-}a]^{+\cdot}$: 415.2818, 416.2944, 417.2975, 418.3100, 419.3131, 420.3256 (monoene: 419.3188, diene: 417.3032, triene: 415.2875).

bis(4-(7-alkyl-2H-benzo[e][1,3]oxazin-3(4H)-yl)phenyl)methane (**C-ddm**). The preparation method is similar to that of C-a except that ratio of reactants used: cardanol (5.00 g, 16.61 mmols), paraformaldehyde (1.00 g, 33.32 mmol), 4,4'-diaminodiphenylmethane (1.65 g, 8.30 mmol) and reaction was heated at a temperature of 90^{o}C for 4h. C-ddm was obtained as orange coloured sticky solid. Yield 85%; FTIR-ATR (diamond crystal/cm^{-1}): 3007, 2920, 2851,1614, 1575, 1513, 1466, 1365, 1276, 1225, 1111, 1086, 1015, 971, 986, and 942.^{1}H-NMR (500 MHz, $CDCl_3$, δ ppm): 0.94 (CH_3,t), 1.35 [(CH_2)n, m], 1.85, 2.07 (CH_2CH=, m), 2.59 (CH_2Ar, t), 2.89 [$CH_2(CH=)_2$, m], 3.83 (s, Ar-CH_2-Ar), 4.55 (s, $ArCH_2N$–), 5.05 (–CH=CH–, dd), 5.40 (m, CH=, CH_2=CH–, –OCH_2N–, –HC=CH_2), 6.60-7.23 (m, ArH); ^{13}C-NMR (125 MHz, $CDCl_3$, ppm): 40.37 ($ArCH_2Ar$), 50.36 ($ArCH_2N$–), 79.77 (–OCH_2N–); LC-MS (ESI Interface-positive ions) $[C\text{-ddm}]^{+\cdot}$:843.5606, 845.5762, 846.5799, 847.5912, 848.5952, 849.6063, 850.6104 (monoene: 850.6376, diene: 846.6063, triene: 842.5750).

tris(4-(7-alkyl-2H-benzo[e][1,3]oxazin-3(4H)-yl)phenyl)methane (**C-trisapm**). The preparation method is similar to that of C-a except that ratio of reactants used: cardanol (1.56 g, 5.18 mmols), paraformaldehyde (0.31 g, 10.36 mmol), Tris-APM (0.50 g, 1.72 mmol) and reaction was heated at a temperature of 90^{o}C for 5h. C-trisapm was obtained as viscous brown oil. Yield 80%; FTIR-ATR (diamond crystal/cm^{-1}): 3007, 2923, 2852, 1657, 1610, 1508, 1256, 1240, 1198, 1041, 1014, 990, and 960; ^{1}H-NMR (500 MHz, $CDCl_3$, δ ppm): 4.46 (s, Ar-CH_2-N-), 5.32-5.38 (m, CH=, CH_2=CH-, -OCH_2N-, HC=CH_2, Ar_3C-H); ^{13}C-NMR (125 MHz, $CDCl_3$, ppm): 50.32 ($ArCH_2N$–), 54.5 (Ar_3CH), 79.52 (–OCH_2N–); LC-MS (ESI Interface-positive ions) $[C\text{-trisapm}]^{+\cdot}$: 1261.8551, 1262.8649, 1263.8689, 1264.8783, 1265.8816, 1266.8904, 1267.8904, 1268.8966 (monoene: 1267.9408, diene: 1261.8938, triene: 1255.8469).

tetrakis(4-(7-alkyl-2H-benzo[e][1,3]oxazin-3(4H)-yl)phenyl)methane (**C-tetraapm**). The preparation method is similar to that of C-a except that ratio of reactants used: cardanol (1.58 g, 5.25 mmols), paraformaldehyde (0.41 g, 13.81 mmol), TAPM (0.50 g, 1.31 mmol) was heated at 90^{o}C for 8 h. C-tetraapm was obtained as a gelatinous brown viscous solid. Yield 74%; FTIR-ATR (diamond crystal/cm^{-1}): 3007, 2921, 2851, 1657, 1607, 1503, 1256, 1240, 1199, 1037, 1014, 990, and 960; ^{1}H-NMR (500 MHz, $CDCl_3$, δ ppm): 1.2-1.59 (m, aliphatic -CH_2 protons), 4.46(s, Ar-CH_2-N-), 5.32-5.38 (m, CH=, CH_2=CH-, -OCH_2N-, HC=CH_2), 6.63-7.26 (m, 28 H, ArH); ^{13}C-NMR (125 MHz, $CDCl_3$, ppm): 49.86 ($ArCH_2N$–), 79.22 (–OCH_2N–); LC-MS(ESI Interface-positive ions) $[C\text{-tetraapm}]^{+\cdot}$: 1619.1887,

1693.0913, 1694.1005 (monoene: 1686.2473, diene: 1678.1847, triene: 1670.1221).

Results and discussion

Preparation and Characterization of Cardanol based Benzoxazine Monomers.

Cardanol is a naturally occurring phenolic compound with C15 alkylene chain at the m-position, generated as a waste during processing of cashew from cashew nut tree. Cardanol used in the current work is a mixture of monoene (39%), diene (18%) and triene (25%), and unidentified product (rest, not isolated) as determined by HPLC (Figure S1). In order to ensure the viability of large scale commercial applications, cardanol was used without any further purification.

TrisAPM, the reduced leuco form to the corresponding pararosaniline hydrochloride salt was synthesized using reduction, while TAPM was synthesized from tetraphenylmethane via two-step process. The first step involved nitration of tetraphenylmethane followed by reduction of nitro to amine groups, Scheme 1.

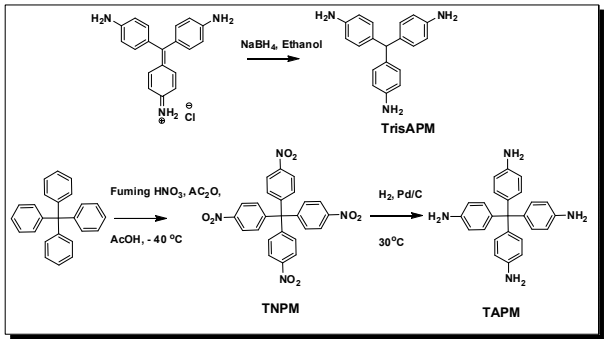

Scheme 1: Preparation of Higher Functionality Amines - TrisAPM and TAPM.

The phenolic group of cardanol was structurally modified to oxazine moiety by reacting with paraformaldehyde and different primary aromatic amines (Aniline, DDM, TrisAPM, TAPM) via Mannich-type reaction to form Bz monomers (Scheme 2). The synthesized benzoxazines are designated based on degree of oxazine functionality as C-a, C-ddm, C-trisapm and C-tetraapm, where 1, 2, 3 and 4 refer to mono-, bis- , tris- and tetra-oxazines respectively. The low value of Brookefield viscosity of cardanol (55.65 mPa.s at 30°C) due to presence of alkylene chain assisted one-pot solventless synthesis for the formation of cardanol based Bz monomers. In addition, further sustainable aspect involves utilization of agrowaste, cardanol as a reactive diluent and by-product of condensation reaction is only water.

The successful synthesis of amines and Bz-monomers was confirmed by FT-IR, ^{1}H- and ^{13}C-NMR spectroscopy. Figure 1 illustrates the FT-IR spectra of tri- and tetra-functional amines namely TrisAPM and TAPM, cardanol and the Bz monomers. TrisAPM and TAPM showed primary amine N-H asymmetric and symmetric and C–N stretch at 3160-3400 cm^{-1} and 1269-1271 cm^{-1} respectively suggesting existence of amino groups (Figure 1a).

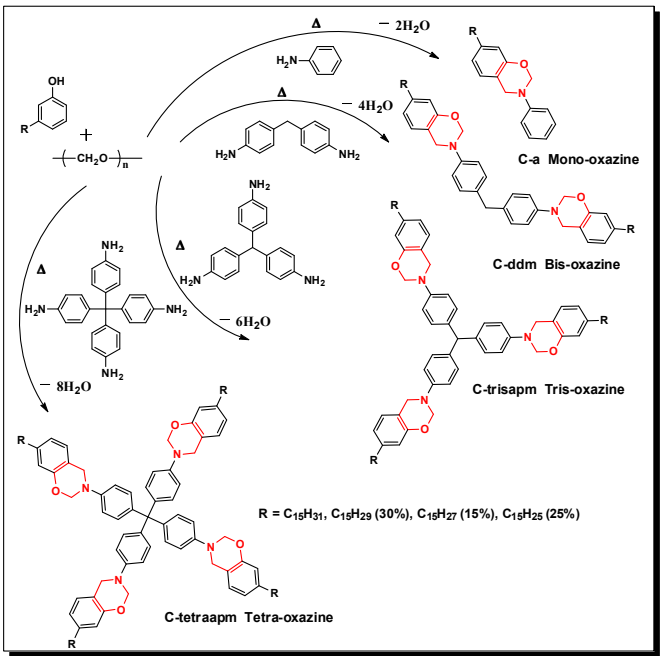

Scheme 2: Preparation of Cardanol based Bz monomers.

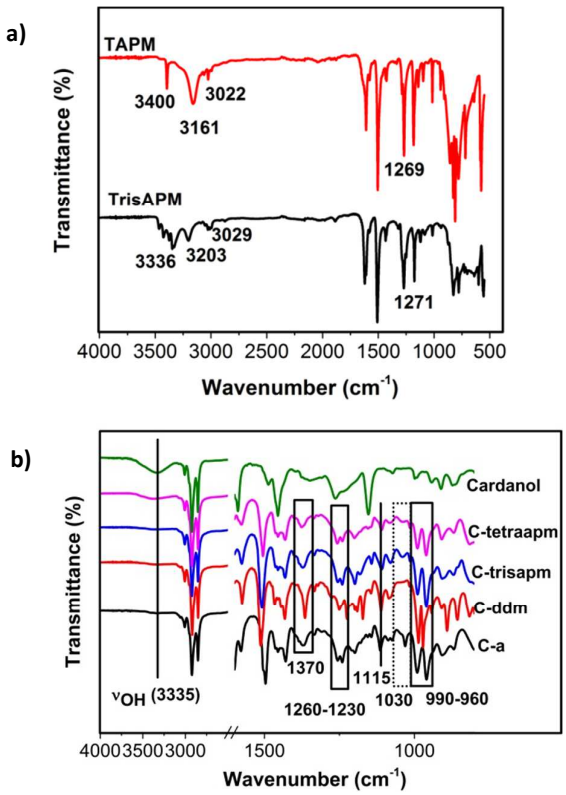

Figure 1. FT-IR spectra of a) Tris-APM and TAPM, b) cardanol and Bz monomers.

Benzoxazine monomers C-a to C-tetraapm, showed absence of O-H and N-H at ~3335, >3161 cm^{-1} (Figure 1b) which suggests complete utilization of cardanol and amine towards formation of oxazine ring. In addition to the stretching bands associated with the aromatic and alkene (3008 cm^{-1}), and aliphatic (2926 and 2854 cm^{-1}) C–H vibrations, other characteristic absorption bands observed in C-a to C-tetraapm, are assigned to the C=C (~ 1600 cm^{-1}), asymmetric and symmetric stretching vibrations of C-O-C (~1245 cm^{-1} and ~1030 cm^{-1}), CH_2 wagging (1370 cm^{-1}), and asymmetric stretching vibrations of C-N-C (1115 cm^{-1}) respectively supporting the presence of double bonds and oxazine ring in Bz monomers (Figure 1b). In cardanol, peak at 990cm^{-1} is ascribed to the C=C-H vinylene C-H out-of-plane bend of alkylene chain. Monomers showed a bimodal peak centered at 990 and 960 cm^{-1} which is attributed to the out-of-plane bending vibrations of C-H bond due to alkylene double bond and oxazine ring respectively.[23]

^{1}H-NMR confirmed the structure of synthesized amines, Tris-APM and TAPM from p-rosaniline hydrochloride and tetra-nitrophenylmethane respectively (Figure S2-S4). In addition to other characteristic aromatic protons, ^{1}H-NMR of TrisAPM showed signal due to Ar_3C-H protons (5.23 ppm, Figure S2). The ^{1}H-NMR analysis of cardanol and the monomers is presented in Figure 2. In comparison to cardanol, C-a to C-tetraapm showed signals at 4.8 ($ArCH_2N$) and 5.3ppm (m, CH=, CH_2=CH–, and $ArOCH_2N$) suggesting formation of oxazine ring due to condensation of amine and hydroxyl group of cardanol in presence of paraformaldehyde. The intensity ratio of signal in Bz monomers at 4.8 (singlet) and 5.3 ppm (multiplet) was found to show a consistent ratio of 1:3 instead of expected 1:1 ratio. The higher integral ratio is accounted due to the resonance of alkylene protons (m, CH=, CH_2=CH–) and Ar_3C-H (in C-trisapm) at similar position as $ArOCH_2N$ ~5.3 ppm as it is clearly evidenced by the appearance of similar signal in cardanol. In case of C-tetraapm this integration ratio was found to be ~ 1:5. Neither altering the reaction time nor elevation of reaction temperature (>90^{o}C) lowered this integration ratio, rather the former led to incomplete reaction and latter resulted in the formation of insoluble polymer. Therefore, in case of synthesis of C-tetraapm, reaction conditions were found to be optimum at >90^{o}C for 8h to eliminate the presence of unreacted starting material. ^{13}C-NMR of Bz monomers showed the presence of $ArCH_2N$ and $ArOCH_2N$ signals at ~50.5 and ~79.4 ppm respectively suggesting formation of oxazine ring. ^{13}C-NMR spectrum of C-ddm is shown in Figure 3 and others are provided in supporting information (Figure S5-7). ^{1}H-NMR of C-tetraapm showed resonance around 3.6 ppm due to $>CH_2$ groups in the Mannich base of dimers/trimers suggesting presence of oligomers. The amount of oligomer in C-tetraapm monomer was calculated by examining the ratio between the integrated intensities of the resonance peaks in ^{1}H-NMR of C-tetraapm. The ratio between the integrated intensity of the methylene units in the benzoxazine ring and the integrated intensity of the methylene units in the oligomer was found to be 1:0.45. Consequently, the amount of oligomer content in C-tetraapm was estimated as 31%. It was reported that the presence of 30% (w/w) of cardanol in petro-based bisbenzoxazine monomer BA-a lowered the onset curing temperature from 142 to 135^{o}C without affecting peak curing temperature.[6] However in our case, the curing temperature is much more affected so we believe in Bz4 the effect on ring opening temperature is due to both oligomeric impurity and neighbouring oxazine rings.

This is further confirmed by appearance of signal at 68.5 and 62.3 ppm in C-tetraapm (^{13}C-NMR, Figure S7). Mass spectrometry of the monomers revealed the existence of molecular ion peak corresponding to the benzoxazine monomer having alkylene chain containing mono-, di-, tri-ene and their mixture.

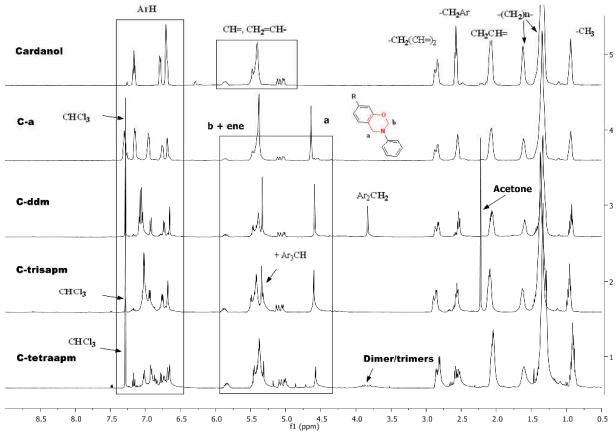

Figure 2. ^{1}H-NMR spectra of cardanol and Bz monomers in $CDCl_3$.

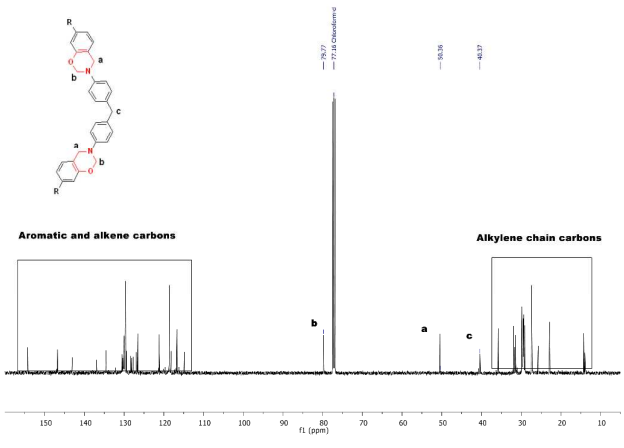

Figure 3. ^{13}C-NMR spectrum of C-ddm in $CDCl_3$.

Curing Behavior of Cardanol based Benzoxazine Monomers.

The curing behavior of Bz monomers (C-a to C-tetraapm) was analyzed and monitored by Differential Scanning Calorimetry (DSC) (Figure 4 and results are summarised in Table 2) and FTIR studies. DSC scans of C-a and C-tetraapm reveal a steady decrease in the initiation of curing temperature (ΔT_i = 85^{o}C) and peak curing

temperature (ΔT_p= 75°C). The number of oxazine moiety per cardanol unit is same in the synthesized homologous series of Bz monomers, therefore this lowering of T_i and T_p is accounted due the neighbouring effect of oxazine moieties. Benzoxazine polymerization is autocatalytic nature therefore the presence of higher number and adjacent oxazine functionalities may promote faster ring opening reaction. The C-tetraapm monomer exhibits T_i of 140°C, and it is, to the best of our knowledge, the first cardanol based Bz monomer with such a lower curing temperature, without any added latent catalyst. However, this lowering may be partly due to existence of oligomers in the monomer.

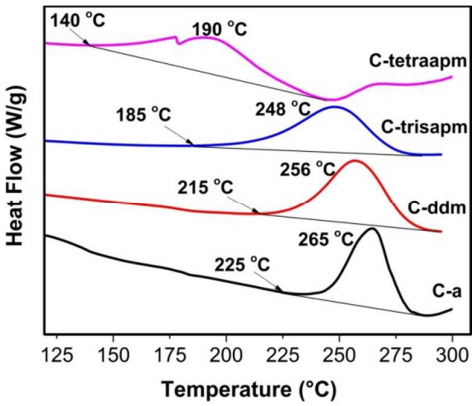

Figure 4. DSC profile of the Benzoxazine Monomers.

The curing study of Bz monomers was also monitored by FTIR using both non-isothermal (Figure S8) and isothermal (Figure S9) heating cycles. The cycle for non-isothermal curing involved heating for 1 h each at 50°C, 100°C, 150°C, 200°C and 210°C for C-trisapm, same cycle was extended to involve 2h heating at 200°C followed by 1 h at 210°C for C-ddm and 1h heating at 220°C, 230°C and 240°C for C-a. In case of C-tetraapm, after 1h curing at 150°C further heating at 160°C and 170°C for one hour each led to completely cured polybenzoxazine. In all samples (Figure S8), it can be observed that peaks characteristic of oxazine functionality (960, 1030 and 1260 cm^{-1}) are intact till 150°C except C-tetraapm which showed diminished intensity and got completely cured at 170°C. In C-a to C-trisapm, as the temperature is increased to 200°C, a marked broadening of peaks, decrease in peak intensity and finally disappearance of characteristic peaks is indicative of oxazine ring opening and completion of curing of the monomer. This ease of ring opening was found to follow the order as C-tetraapm> C-trisapm> C-ddm> C-a. Similarly, isothermal curing studies (Figure S9), revealed that increasing the functionality of the monomers led to a decrease in the cure duration. The monomers C-tetraapm, C-trisapm, C-ddm and C-a could be completely cured in 0.5, 4h, 5h and > 10h respectively.

To provide further understanding, DFT calculations were carried out to give more insight into the different extent of polymerization of C-a to C-tetraapm. All the calculations were carried out using Gaussians 09 package.[40] The geometry optimizations were carried out using Becke's three parameters hybrid functional and Lee-Yang-Parr exchange correlation functional (B3LYP)[41-43] and 6-31+G** basis set[44-45] was used for all the atoms. Harmonic vibrational frequencies were calculated to characterize the nature of the stationary points. The optimized structures of monomers are shown in Figure 6. It is understood that the breaking of -O-CH_2- bond is the key step for the autocatalytic polymerization of benzoxazine. Therefore, the bond length and the torsional stress at the -O-CH_2- bond is the most important factor to dictate its bond dissociation. Interestingly, the O-CH_2 bond distance is 1.45 Å in the C-tetraapm whereas 1.42 Å in C-a to C-trisapm (Figure 5). Therefore, the elongated bond in C-tetraapm might be helping the bond dissociation process thus the formation of hydroxyl species, which in turn favours the polymerization. The torsional stress can be understood from the torsional angle (ϕ, Figure 6a) of C-O-H_2C-N planes. The values are -51.7, -50.0, -49.8, -45.0 for C-a, C-ddm, C-trisapm and C-tetraapm respectively (Figure 6a). Thus the value is lowering from C-a to C-tetraapm, suggesting higher the torsional strain which lowers the bond dissociation energy.

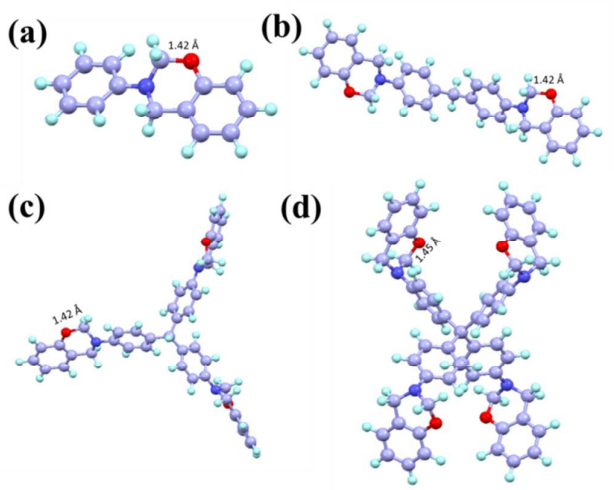

Figure 5. Optimized structures of (a) C-a, (b) C-ddm, (c) C-trisapm and (d) C-tetraapm.

We have calculated the strain energy of the O-CH_2 bond of the monomers by calculating the formation of free energy when the cyclic part is converted to its acyclic counterpart, balancing the number of atoms and bonds in the cyclic versus the acyclic compound. Here, the O-CH_2 bonds of the cyclic system is converted to its acyclic counterparts by hydrogenating the O-CH_2 bonds and converting into –OH and –CH_3 fragments as shown in Figure 6b. Here hydrogenation energy is considered to be the bond strain energy as they are reported to be very much comparable.[46,47] The strain energy is calculated to be highly favourable (exothermic) for C-tetraapm in comparison to C-a, C-ddm and C-trisapm. The calculated strain energy values are -19.14, -41.71, -61.89 and -86.41 kcal/mol for C-a, C-ddm, C-trisapm and C-tetraapm respectively. As the strain energy is much higher for the higher oxazine family (C-

tetraapm) thus favors the autocatalytic polymerization at lower temperature which supports our experimental findings.

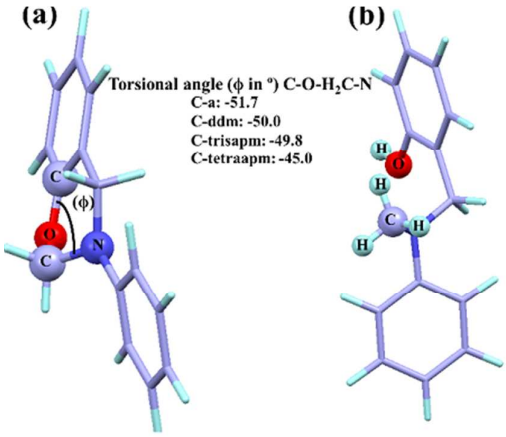

Figure 6. (a) Torsional angle (ϕ) of C-O-H_2C-N planes for oxazines, (b) Hydrogenated product.

As the curing of monomer proceeds, oxazine ring undergoes ring opening reaction to form hydroxyl and amino groups which form H-bonding among polymer chains. In polybenzoxazines, there is possibility of existence of both intermolecular (between two phenolic hydroxyl groups) and intramolecular (between phenolic hydroxyl groups and phenolic hydroxyl groups and/or nitrogen atoms on the Mannich bridge) hydrogen bonding. The extent and nature of H-bonding will be different in PC-a to PC-tetraapm and the probability of their occurrence will be more in PC-tetraapm than PC-a (Figure 7). It is an important aspect in dictating the polymer thermo-mechanical properties in polybenzoxazines. FTIR spectrum of polybenzoxazines PC-a to PC-tetraapm showed a red shift and broadening in absorption of phenolic O–H stretching vibration band (centered at 3440 cm^{-1}) suggesting an increase in extent of H-bonding sites (inset Figure 7) in PC-tetraapm over PC-a. The polymer PC-tetraapm may relatively form more H-bonding sites due to close vicinity of neighbouring oxazine rings over others.

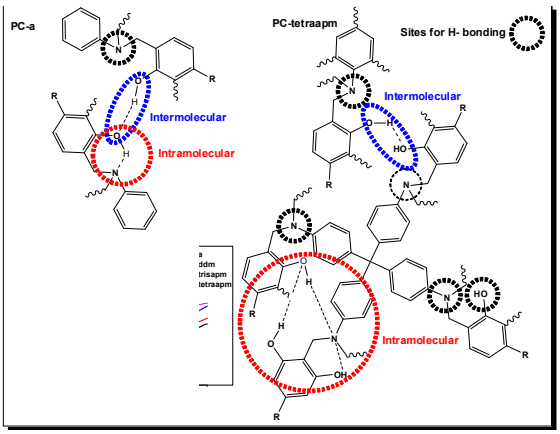

Figure 7. Probable sites of H-bonding in PC-a and PC-tetraapm (inset shows FTIR spectra of Cured PBz Resins)

Rheological property of monomers, thermo-mechanical and thermal stability of Cured PBz Resins.

Ease of polymer processing is strongly dependant on the viscosity, which, therefore, is an important parameter in deciding its applicability and viability. The difference in liquefaction and gelation temperatures gives an estimate of the processing window available as in this particular temperature range polymer by the virtue of its low viscosity can be easily molded or compounded. Rheological studies were performed in order to ascertain gelation behaviors of cardanol based benzoxazines so as to get an estimate of the effect of increasing functionality on processability of monomers (Figure 8a). The complex viscosity curve showed no noticeable liquefying point as opposed to solid powdered monomers due to liquid to semi-viscous nature of cardanol based monomers at room temperature. In this series higher functionality resins (C-ddm to C-tetraapm) showed a decrease in gelation temperature with increase in number of oxazine rings as can be observed from the complex viscosity plots. In case of C-a, the complex viscosity is really low due to less rigid structure and the presence of long alkylene chain which contributes in substantial lowering of the viscosity (inset Figure 8a). PC-a also showed a marginal viscosity build up mainly due to its linear structure.

The dynamic mechanical thermal analysis (DMTA) of cardanol based polybenzoxazines was carried out to measure variation of glass transition temperature (T_g) and moduli with enhanced oxazine functionality in monomers. T_g in particular is an effective measure of the parameters like polymeric backbone rigidity and crosslink density. In this case an increase in oxazine functionality in the monomer is expected to result in enhanced cross link density which in turn is expected to increase the corresponding T_g values and improve the storage moduli values. Storage modulus values are in the range of 3.6 - 66.5MPa (at rubbery plateau). As it can be observed in Figure 8b, storage moduli behavior exhibits a marked improvement in the rubbery plateau for PC-tetraapm to PC-ddm when compared to the PC-a. This is indicative of a high cross-linking density in former in comparison to PC-a which is in analogy to its linear structure due to mono-oxazine nature of monomer. The storage modulus determined from rheology data of structural analogous bisoxazine based on 4,4'-diaminodiphenylmethane with cardanol (C-ddm) or petro-based phenol were compared. Cardanol based monomer C-ddm showed a value of 45.0 MPa while phenol showed a much lower value of 7 MPa.[48] The only difference in the two structure is the presence of C15 alkylene chain (in C-ddm), which may be enhancing its ability to resist intermolecular slippage of polymer structures. T_g values can be given by the damping factor maxima in DMA test (Figure 8d). The T_g values was found to show a progressive increase with increasing oxazine functionality in the monomer, which is due to the increase extensive hydrogen bonding in PC-tetraapm vs PC-a, which reduce the chain mobility. This is also confirmed by FTIR studies (inset of Figure 7) which supports the presence of neighboring oxazine ring led to enhancement in H-bonding sites and thereby increase in T_g values.

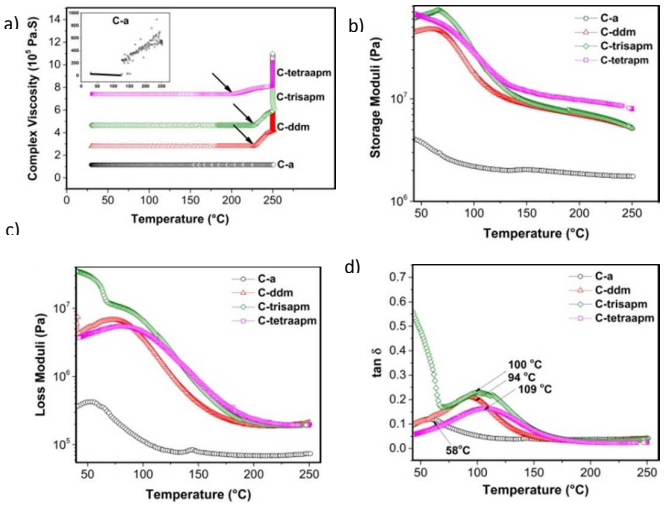

Figure 8. Rheological and thermomechanical properties of monomers and polymers a) Complex viscosity; b) Storage moduli; c) Loss moduli; d) Damping Factor (tan δ).

In an ideal mode, the topology of network formation will orient along the direction of oxazine rings which may be dictated according to the geometrical structure of the monomer. However, network formation successively proceeds in several stages including oligomerization, branching, gelation and with the eventual formation of highly crosslinked network. The difference in gelation temperatures and thermo-mechanical properties of C-trisapm were found to be unique as compared to C-ddm and C-tetraapm due to its different monomer architecture and thereby different cross-linking network formation. We believe that C-ddm and C-tetraapm will extend in two and four different directions respectively, while C-trisapm will grow in three directions affecting the network formation.

Considering PBz as lightly cross-linked material, cross link density calculations were performed based on the data obtained from the storage modulus of the rubbery region following the equation from statistical theory from elastic mechanics.[49]

$$G' = \emptyset \upsilon RT$$

where, G' refers to the storage modulus at the rubbery plateau, ϕ is the front factor taken as unity for ideal rubbers, R is the gas constant and T is the absolute temperature. The cross link density value (ν) i.e. number of moles of network chains per unit volume of the cured polymer or concentration of network chains is calculated in Table 1. Petro-based PBz based on bisoxazines, bisphenol-A/aniline or linear aliphatic diamines[49] showed a ν of 1.1 -7.4x 10^{-3}mol/cm^3 whereas PC-a to PC-tetraapm showed 0.7-3.1x 10^{-3}mol/cm^3. PC-tetraapm showed the highest cross link density, in comparison to PC-a. A low cross link densities of cardanol based counterparts in comparison to petro-source can be attributed to the presence of longer alkyl side chain. PC-a to PC-tetraapm showed a simultaneous decrease in value of molecular weight between cross links from 1530 to 310 g/mol. A nearly five-fold decrease in molecular weight between cross links was obtained as structure was changed from C-a to C-tetraapm, suggesting a good equivalence among the formed polymer network which differ each other by the number of linking benzene moiety from 1 to 4.

Table 1. Crosslink Densities of PBz resins and LSS of Steel Bonded joints.

Polymer	Storage Modulus (G')/ MPa at T_g+50°C	Crosslink density, ν (ν *10^3mol/cm^3)	Density (ρ) (mol/cm^3)	Molecular weight between crosslinks (Mc*10^{-3} g/mol)	LSS (Kg/ cm^2)
PC-a	2.18	0.66	1.05	1.53	26
PC-ddm	9.09	2.62	1.06	0.41	79
PC-trisapm	9.50	2.70	1.04	0.39	100
PC-tetraapm	11.30	3.13	0.99	0.31	n.d.

High glass transition temperatures of cardanol based polybenzoxazines compared to relatively lower cross link density values is due to existence of extensive inter- and intra- molecular hydrogen bonding contributing to the enhanced rigidity of the system.

Lap shear strength (LSS) is a measure of adhesive strength of the polymer, with a higher value indicative of higher adhesive strength. LSS of cardanol based polybenzoxazines followed the order PC-a<PC-ddm<PC-trisapm which is mediated by the extent of H-bonding (inset of Figure 7) and cross-linking density (Table 1). PC-tetraapm was not studied for adhesive applications due to commercially unsustainable synthetic procedure of TAPM.

Thermal stability of the cured monomers was analyzed by Thermogravimetric Analysis (TGA) as shown in Figure 9 and Table 2. TGA revealed a steady increase in thermal stability (T5%, Δ= 36°C), char yield (700°C, Δ= 24%) and Limiting oxygen index (LOI) values (700°C, Δ= 8%) for mono to tetraoxazine based polymer (PC-a to PC-tetraapm) respectively, suggesting the formation of a higher cross-linked network due to the close vicinity of oxazine rings. Higher aromatic content in higher functionality based oxazine polymers account for higher char yield (PC-ddm to PC-tetraapm: 32-37%) than lower aromatic content mono-oxazine based polymer (PC-a: 13%). The LOI value was found to be greater than 23, which is considered to be suitable for application of these polymers in areas necessitating flame retardance. The calculated LOI values of PC-ddm to PC-trisapm reflect values as 28-31 indicating high flame retardancy of higher functionality monomers due to higher aromatic content.

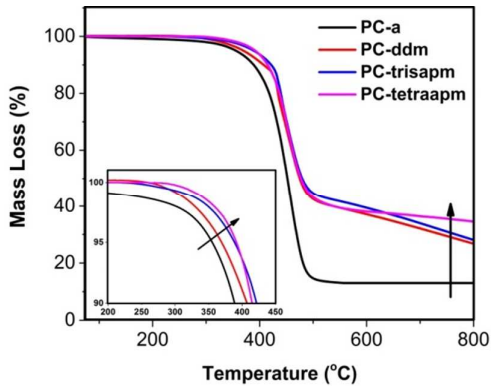

Figure 9. TGA profile of Cured PBz Resins.

Benzoxazine	Curing Exotherm (°C)		Thermal Stability of cured Resin (°C)		LOI[a,46]	Glass Transition Temperature (°C)
	T_i	T_p	$T_{5\%}$	Char Yield (%)		T_g
C-a	225	265	355	13	23	58
C-ddm	215	256	369	32	28	94
C-trisapm	185	248	388	34	29	100
C-tetraapm	140	190	391	37	31	109

[a]LOI: Limiting oxygen index was determined using Van Krevelan and Hofytzer equation,[50] LOI =17.5 + 0.4 (Char yield, %).

Conclusions

A homologous series of cardanol based benzoxazine monomers (C-a to C-tetraapm) were designed and synthesized, where the degree of oxazine functionality is varied from 1 to 4. Interestingly, a strong correlation between the number of oxazine rings and the properties of the monomer and polymer was observed. With the increase in number of oxazine rings, a lowering in initiation of thermal curing temperature form 225 to 140°C was observed, which is lowest among the pristine Bz monomers reported till date. While the present study highlights the structural modification of Bz monomer, it is believed that through appropriate functionalization of the monomer, further lower of curing temperature is possible. The glass transition temperature and storage modulus was found to increase from 58 to 109°C and 3.6 - 66.5MPa respectively from PC-a to PC-tetraapm suggesting an important role on nature of monomer, degree and close vicinity of functionality which affect cross-linking density and thereby the polymer properties. Thermal stability, LOI and LSS was found to increase from the PC-a to PC-tetraapm prospecting their candidature in flame retardant, composite and adhesive applications. Multi-oxazine Bz monomers may prove useful for tailoring scientifically and technologically interesting materials by suitable choice of phenol and/or amine modulating the structure of monomer, hence properties of PBz matrix.

Acknowledgements

The authors (SS, BL) would like to acknowledge the financial support from Shiv Nadar University and DST/BL/2014/15 and are thankful to Dr. P. K. Roy (DRDO), Dr. Dharmesh Gala (Anton Paar) and Dr. P. Mukhopadhyay (AIRF, JNU) for providing assistance in characterization facility. We are thankful to SCCPL®, India for providing cardanol.

Notes and references

‡ Supporting Information: HPLC trace of cardanol. ^{1}H-NMR spectra of TrisAPM, TNPM and TAPM. ^{13}C-NMR spectra for the monomers of C-a, C-trisapm and C-tetraapm. FTIR spectra of isothermal and non-isothermal curing studies.

1 N. N. Ghosh, B. Kiskan and Y. Yagci, *Prog. Polym. Sci.* 2007, **32**, 1344.
2 X. Ning and H. Ishida, *J. Polym. Sci., Part A: Polym. Chem.* 1994, **32**, 1121.
3 M. Arslan, B. Kiskan and Y. Yagci, *Macromolecules*. 2015, **48**, 1329.
4 W.– H. Hu, K.– W. Huang, C.– W. Chiou and S.– W. Kuo, *Macromolecules*, 2012, **45**, 9020.
5 M. G. Mohamed, K. –C. Hsu and S. –W. Kuo, *Polym. Chem.* 2015, **6**, 2423.
6 Handbook of Benzoxazine Resin. H. Ishida and T. Agag, Eds., Amsterdam (2011), pp.675-678.
7 A. Chernykh, T. Agag and H. Ishida, *Macromolecules*, 2009, **42**, 5121.
8 D. D. Demir, B. Kiskan and Y. Yagci, *Macromolecules*, 2011, **44**, 1801.
9 R. S. Kumar and M. Alagar, *RSC Adv.* 2015, **5**, 33008.
10 A. A. Alhawaige, T. Agag, T and H. Ishida, *Biomacromolecules*, 2013, **14**, 1806.
11 G. Lligadas, A. Tüzün, J. C. Ronda, M. Galià and V. Cádiz, *Polym. Chem.* 2014, **5**, 6636.
12 P. Thirukumaran, A. Shakila and S. Muthusamy, RSC Adv. 2014, **4**, 7959.
13 P. Thirukumaran, A. S. Parveen, M. Sarojadevi, *ACS Sustainable Chem. Eng.* 2014, **2**, 2790.
14 P. Thirukumaran, A. S. Parveen, M. Sarojadevi, *New J. Chem.* 2015, **39**, 1691.
15 N. K. Sini, J. Bijwe and I. K. Varma, *J. Polym. Sci. Part A: Polym. Chem.* 2014, **52**, 7.
16 N. K. Sini, J. Bijwe and I. K. Varma, *Polym. Degrad. Stab.* 2014, **109**, 270.
17 A. Van, K. Chiou and H. Ishida, *Polymer*. 2014, *55*, 1443-1451.
18 H. Xu, Z.Lu and G. Zhang, *RSC Adv.* 2012, *2*, 2768-2772.
19 H. Xu, W. Zhang, Z. Lu and G. Zhang, *RSC Adv.*, 2013, **3**, 3677.
20 S. Li, T. Zhou, X. Liu and M. Tao, *Des. Monomer Polym.* 2014, **17**, 40.
21 C. F. Wang, J. Q. Sun, X. D. Liu, A. Sudo and T. Endo, *Green Chem.* 2012, 14, 2799.
22 22 M. Comi, G. Lligadas, J. C. Ronda, M. Galia and V. Cadiz, *J. Polym. Sci. Part A: Polym. Chem.*, 2013, **51**, 4894.
23 B. Lochab, S. Shukla and I. K. Varma, *RSC Adv.* 2014, **4**, 21712.
24 B. Lochab, I. K. Varma and J. Bijwe, *J. Therm. Anal. Calorim.* 2010, **102**, 769.
25 E. Calo, A. Maffezzoli, G. Mele, F. Martina, S. E. Mazzetto, A. Tarzia and C. Stifani, *Green Chem.* 2007, *9*, 754-759.
26 B. S. Rao and A. Palanisamy, *Eur. Polym. J.* 2013, **49**, 2365.
27 2B. Lochab, I. K. Varma and J. Bijwe, *J. Therm. Anal. Calorim.*, 2012, **107**, 661.

28 B. S. Rao and A. Palanisamy, *React. Funct. Polym.* 2011, **71**, 148.
29 C. F. Wang, C. H. Sun, J. Q. Zhao, S. Q. Huang, X. D. Liu and T. Endo, *J. Polym. Sci. Part A: Polym. Chem.* 2013, **51**, 2016.
30 C. Liu, D. Shen, R. M. Sebastián, J. Marquet and R. Schönfeld, *Polymer*. 2013, **54**, 2873.
31 M. Baqar, T. Agag, R. Huang, J. Maia and S. Qutubuddin, *Macromolecules*, 2012, **45**, 8119.
32 R. Andreu, J. A. Reina and J. C. Ronda, *J. Polym. Sci. Part A: Polym. Chem.* 2008, **46**, 3353.
33 B. Lochab, I. K. Varma and J. Bijwe, *J. Therm. Anal. Calorim.* 2013, *111*, 1357-1364.
34 H. Wang, J. Wang, X. He, T. Feng, N. Ramdani, M. Luan, W. Liu and X. Xua, *RSC Adv.*, 2014, **4**, 64798.
35 C. W. Chang , C. H. Lin, H. T. Lin, H. J. Huang, K. Y. Hwang and A. P. Tu, *Eur. Polym. J.*, 2009, **45**, 680.
36 D. Wang, B. Li, Y. Zhang and Z. Lu, *J. Appl. Polym. Sci.*, 2013, **127**, 516.
37 T. Zhang, Jun Wang, T. Feng, H. Wang, N. Ramdani, M. Derradji, X. Xu, W. Liu and T. Tang, *RSC Adv.*, 2015, **5**, 33623-33631
38 H. Houjou, T. Koga, M. Akiizumi, I. Yoshikawa and A. Koji, *Bull. Chem. Soc. Jpn.* 2009, **82**, 730.
39 J. Wang, Y. Masui and M. Onaka, *Polym. Chem.* 2012, **3**, 865.
40 Gaussian 09, Revision C.01, M. J. Frisch, G. W. Trucks, H. B. Schlegel, G. E. Scuseria, M. A. Robb, J. R. Cheeseman, G. Scalmani, V. Barone, B. Mennucci, G. A. Petersson, H. Nakatsuji, M. Caricato, X. Li, H. P. Hratchian, A. F. Izmaylov, J. Bloino, G. Zheng, J. L. Sonnenberg, M. Hada, M. Ehara, K. Toyota, R. Fukuda, J. Hasegawa, M. Ishida, T. Nakajima, Y. Honda, O. Kitao, H. Nakai, T. Vreven, J. A. Jr. Montgomery, J. E. Peralta, F. Ogliaro, M. Bearpark, J. J. Heyd, E. Brothers, K. N. Kudin, V. N. Staroverov, R. Kobayashi, J. Normand, K. Raghavachari, A. Rendell, J. C. Burant, S. S. Iyengar, J. Tomasi, M. Cossi, N. Rega, J. M. Millam, M. Klene, J. E. Knox, J. B. Cross, V. Bakken, C. Adamo, J. Jaramillo, R. Gomperts, R. E. Stratmann, O. Yazyev, A. J. Austin, R. Cammi, C. Pomelli, J. W. Ochterski, R. L. Martin, K. Morokuma, V. G. Zakrzewski, G. A. Voth, P. Salvador, J. J. Dannenberg, S. Dapprich, A. D. Daniels, Ö. Farkas, J. B. Foresman, J. V. Ortiz, J. Cioslowski, D. J. Fox, Gaussian, Inc., Wallingford CT, 2009.
41 A. Becke, Density-functional thermochemistry. III. The role of exact exchange. *J. Chem. Phys.* 1993, **98**, 5648.
42 A. Becke, Density-functional thermochemistry. III. The role of exact exchange. *J. Chem. Phys.* 1996, **104**, 1040.
43 C. T. Lee, W. T. Yang and R. G. Parr, *Phys. Rev. B.* 1988, **37**, 785.
44 T. Clark, J. Chandrasekhar, G. W. Spitznagel and P. V. R. Schleyer, *J. Comput. Chem.* 1983, **4**, 294.
45 P. C. Hariharan and J. A. Pople, *Theor. Chim. Acta.* 1973, *28,* 213−222.
46 T. Dudev and C. Lim, *J. Am. Chem. Soc.* 1998, **120**, 4450.
47 R. D. Bach, *J. Am. Chem. Soc.* 2009, **131**, 5233.
48 R. Huang, S. O. Carson, J. Silva, T. Agag, H. Ishida and J. M. Maia, *Polymer*, 2013, **54**, 1880.
49 D. J. Allen and H. Ishida, *J. Appl. Polym. Sci.* 2006, **101**, 2798.
50 C. L. Chiang and M. C. Ma, *Polym. Degrad. Stab.* 2004, **83**, 207.